MEAN VOLUME RADIUS ESTIMATES FROM AIRCRAFT, RADIOMETER, AND DOPPLER RADAR OBSERVATIONS DURING THE AIRS FIELD PROJECT

I.Gultepe, G.A. Isaac, and D. Hudak
Cloud Physics Research Division,
Meteorological Service of Canada,
4905 Dufferin St., Toronto, Ontario M3H 5T4, Canada

S. Sekelsky
Microwave Remote Sensing Laboratory
Department of Electrical & Comp. Eng.
University of Massachusetts, Amherst, MA 01003, USA

1. INTRODUCTION

The purpose of this work is to estimate mean volume radius (r_{mvr}) from in-situ and remote sensing observations collected during the Alliance Icing Research Study (AIRS). This project took place over the Ottawa, Ontario and Mirabel, Quebec regions during the winter of 1999-2000 (Isaac et al, 2001). The r_{mvr} is defined as

$$r_{mvr} = [\ \sum_{i}^{j} n_i r_i^3 / \sum_{i}^{j} n_i\ ]^{1/3}, \qquad 1$$

where n_i is the number concentration and r_i is the size at each bin, with j representing the number of bins.

2. OBSERVATIONS

Concurrent measurements of aircraft, Doppler radar and microwave radiometer observations for Dec. 16 1999 and Jan. 25 2000 were used in the analysis. The cases are chosen based on the in-situ observation of liquid phase particles and significant icing experienced within the clouds. Moderate and severe icing events occurred at 1757-2151 UTC on Dec. 16 and at 1903-2336 UTC on Jan. 25, respectively. The following sections describe measurements from various instrument platforms.

2.1 In-situ measurements

The droplet number concentration (N_d) and ice crystal number concentration (N_i) were obtained at size ranges of 2-47 and 5-95 μm from two Particle Measuring Systems (PMS) Forward Scattering Spectrometer Probes ($FSSP_{96}$-100 and $FSSP_{124}$-100), and at 25-800 μm from PMS two dimensional-cloud (2D-C) probe measurements, respectively. The liquid water content (LWC) was obtained from measurements of the King, FSSP-100, and Nevzorov probes. The Nevzorov probe LWC and total water content (TWC) measurements are accurate to within 10-15% (Korolev et al., 1998). Temperature was measured by reverse flow temperature probe to an accuracy of ±1°C.

2.2 Doppler radar measurements

Doppler radar measurements at Mirabel Airport were collected by the University of Massachusetts Cloud Profiling Radar System (CPRS) and a X band McGill vertical pointing radar (VPR) at X-band. The range resolution for the X band radar is 37.5 m and the sensitivity of Z is about -25 dBZ at 1 km. The CPRS operates simultaneously at 33 GHz (Ka-band) and 95 GHz (W-band), but here only the Ka-band channel data is used. The reflectivity (dBZe) calibration is approximately ±1 dB. The Doppler resolution is approximately ±5 cm s^{-1}. The sensitivity is approximately –40 dBZe at 5 km for the integration time used for the AIRS data.

Corresponding author address: Dr. Ismail Gultepe, Cloud Physics Research Division, Meteorological Service of Canada (MSC), Toronto, Ont. M3H 5T4, Canada

2.3 Microwave radiometer measurements

The Radiometrics WVR-1100 microwave radiometer (MWR) measurements at two frequencies 23.8 (K-band) and 31.4 GHz (Ka band) were collected over Mirabel airport. These two frequencies allow simultaneous determination of integrated water vapor and integrated liquid water content (LWP) along a selected path. The uncertainty in the MWR measurements of LWP was about 15-25% (Personnel communication with F. Solheim).

3. METHOD

The N_d, LWC, Doppler velocities (V_d), reflectivity (Z), liquid water path (LWP), and cloud physical thickness (dz) were used to obtain r_{mvr} profiles from four methods for two cases. Glaciated regions are not considered and were removed from the analysis based on in-situ measurements. Liquid, mixed, and glaciated cloud regions were identified with the aircraft data following the methodology of Cober et al, 2001a,b). The methods, which utilized theoretical derivations, empirical relationship, and observations, are summarized below. The time period used in the averaging of in-situ data is taken as 60 minutes but for the Ka band radar, a 20 minutes time period was used.

3.1. Based on Doppler velocity measurements (DV)

This method relates r_{mvr} to Doppler velocities (V_d), and assumes that the mean V_d is negligible over a 20 minute scale (Kato et al, 2001):

$$r_{mvr} \cong 13.2\overline{ww}^{1/4} \qquad 2$$

where the vertical air velocity (w) variance (ww) is assumed to be approximated by V_d variations (V_dV_d). The V_d variations are obtained from the Ka band radar measurements at 500 m intervals over 20 minute time intervals. The measurements at a 10-degree elevation angle for the Dec. 16 case are converted to represent a 90-degree elevation angle.

3.2 Using aircraft and radiometer measurements (AR method)

Using an equation given by Gultepe et al (1996), r_{mvr} is obtained as

$$r_{mvr}^3 = \frac{1}{\Delta z}\frac{3x10^6\, LWP}{4\pi N_d}, \qquad 3$$

where N_d, LWP and r_{mvr} are in the units of cm^{-3}, g m^{-2}, and μm. LWP is obtained from the MWR measurements. N_d in Eq. 3 can be estimated from N_d versus T relationship (Gultepe et al, 2002) or aircraft measurements. N_d is given as:

$$N_d = -0.0905T^2 + 1.62T + 175.1 \qquad 4$$

where N_d and T have units of cm^{-3} and °C, respectively.

3.3 Using aircraft measurements and empirical relationships (AE method)

Gultepe et al (2001) showed that the extinction coefficient is related to both LWC and N_d as

$$\log(\sigma_{ext}) = 0.7357 + 0.4653\log(LWC) + 0.5295\log(N_d) \quad 5$$

where N_d is obtained either directly from aircraft observations or from an N_d-T relationship (Eq. 4). Using the results of Gultepe et al. (2002), the LWC-T relationship is also obtained as

$$LWC = 5x10^{-5}T^2 + 0.0058T + 0.1525 \; . \quad 6$$

Then, using Eqs. 5 and 6,

$$r_{mvr} = k^{1/3}3LWC/2\rho_w\sigma_{ext} \; . \quad 7$$

where k is taken as a constant value of 0.7 for stratiform clouds.

3.4 Using aircraft and Doppler radar measurements (ADR method)

The r_{mvr} is also obtained from an equation given by Kato et al (2001):

$$r_{mvr} = k^{1/3} r_m^{-2/9} \left(\frac{3LWC}{4\pi\rho N_d} \right)^{1/3} \left(\frac{\pi\rho Z}{48LWC} \right)^{2/27} \quad 8$$

where LWC and N_d are obtained from the LWC-T (Eq. 6) and the N_d-T (Eq. 4) relationships. The r_m is the median radius. The reflectivity factor (Z) values from Doppler radar measurements are estimated at 500 m intervals over a 20 minute time scale.

3.5 Using optical array probes (OP method)

The phase of particles is obtained using the measurements of the hot-wire LWC probes, the Rosemount icing detector, and the optical probes. When the voltage-change rate of the Rosemount icing detector (RID) is greater than 2 mV/s, the LWC values from various probes is greater than 0.005 g m^{-3}, and there is a negligible TWC-LWC difference (<0.01 g m^{-3}), then the FSSP measurements are used to obtain r_{mvr}.

4. RESULTS AND CONCLUSIONS

Fig. 1 shows the radiometer LWP time series for both days collected at Mirabel. In general, the LWP for the Jan. 25 case was higher than the Dec.16 case. Drizzle size droplets on Dec.16 were observed at the surface making the radiometer measurements inaccurate after 19:00 UTC. The cloud particle imager (CPI) probe data on this day indicated that some droplet diameters have sizes larger than 100 μm. Also, drizzle size droplets occasionally were observed for the Jan. 25 case (Isaac et al., 2001).

An in-situ time series for the Dec. 16 case is shown in Fig. 2. Overall, the values of LWC and N_d for the Dec. 16 case were larger than those of the Jan. 25 case (not shown). For the Jan. 25 case, there was a high LWC region at about 22.30 UTC coincident with a heavy icing region.

Figs. 3a and 3b show the Ka band radar Z and V_d values, respectively, at 21:29 UTC for the Jan. 25 case for a 20 minute time intervals. Highly turbulent regions were indicated by large spectral width values (<1 m s^{-1}) at about 5 km where the Z values were low. At 19:31 UTC on Dec. 16 case (not shown), large V_d values at about 700 m and 2000 m heights matched the icing region that was indicated by the in-situ data.

Fig. 4 shows an example for a 30 s average of particle measurements from various optical probes on Jan. 25. It is found that, when droplets with sizes greater than 30 micron are not considered, Z of the droplets is about –33 dBZ. For ice crystals, Z is 9 dBZ. Ice crystals were considered as the equivalent spheres in Z calculation. Approximately 1 hour later, the particle spectra had peaks near 100 micron (Isaac et al, 2001) in the region where severe icing was encountered.

Figs. 5 and 6 show the profiles of $r_{mvr,}$ obtained using the methods described above, for the Dec. 16 and Jan. 25 cases, respectively. The lines in these figures are strongly dependent upon the assumptions used and the accuracy of the measurements. In general, the results from the various techniques are comparable. However, this is suprising in the case of Eq. 8 where the relectivity was dominated by ice crystals, while the equation assumes only liquid particles present. Obviously, the use of empirical relationships (Eqs. 4-7) must be carefully examined on a case by case basis.

Mixed phase clouds were very commonly observed during AIRS (see Isaac et al., 2001), being detected approximately 50% of the time. When ice particles are present, the contribution of the ice to the Z values can be significant, as is indicated in Fig. 4. The use of a polarization radar, and such parameters as deplorization ratio (Sassen et al, 1990), may help to identify cases where reflectivity is dominated by ice particles. This would help resolve some of the uncertainties in applying Eq. 2 and 8. Certainly, if r_{mvr} is to be estimated using remote sensing techniques, the problem of screening the data for glaciated and mixed phase clouds must be overcome. Better empirical relationships that will work in clouds with ice crystals must also be developed and tested.

Acknowledgements: Authors would like to thank to S. G. Cober, J. W. Strapp, Z. Vokovich, F. Fabry and P. Rodrigez for helping during course of this study, and to other MSC and NRC personnel for the planning of the field project and aircraft instruments installation. This work was supported by MSC, NRC, TC, FAA, Boeing, Canadian National Search and Rescue Secretary, and NASA.

REFERENCES:

Cober, Stewart G., George A. Isaac, Alexei V. Korolev, J. Walter Strapp, 2001a: Assessing Cloud-Phase Conditions. J. Appl. Met., 40, 1967–1983.

Cober, S. G., G. A. Isaac, A. V. Korolev, 2001b: Assessing the Rosemount icing detector with in-situ measurements. *J. Atmos. Ocean. Tech.*, 18, 515-528.

Gultepe, I., G. A. Isaac, and S. G. Cober, 2002: Cloud liquid water content versus temperature relationships for three Canadian field projects. *Annales Geophyscae, Accepted*.

Gultepe, I., G. A. Isaac, and K. Strawbridge, 2001:Variability of cloud microphysical and optical parameters obtained from aircraft and satellite remote sensing during RACE. *Inter. J. Climate,* 21, 4, 507-525.

Gultepe, I., Isaac, G. A., Leaitch, W. R., and Banic, C. M., 1996: Parameterization of marine stratus microphysics based on in-situ observations: Implications for GCMs. *J. Climate,* 9, 345-357.

Isaac, G. A., S.G Cober, J. W. Strapp, A. V. Korolev, A. Tremblay, and D. L. Marcotte, 2001: Recent Canadian research on aircraft in-flight icing. *Canadian Aeronautics and Space Journal*, 47, 213-221.

Kato, S., G.G. Mace, E. E. Clothiaux, J. C. Liljegren, R. T. Austin, 2001: Doppler radar derived drop size

distributions in liquid water stratus clouds, *J. Atmos. Sci.,* 58, 2895-2911.

Korolev, A. V., J. W. Strapp, G. A. Isaac, and A. N. Nevzorov, The Nevzorov airborne hot-wire LWC-TWC probe: Principals of operation and performance characteristics. *J. Atmos. Ocean. Tech.*, 15, 1495-1510.

Sassen, K., C. J. Grund, J. D. Spinhirne, M. M. Hardesty, and J. M. Alvarez. 1990: The 27-28 October 1986 FIRE IFO cirrus case study: A five lidar overview of cloud structure and evolution. *Mon. Wea. Rev.*, **118**, 2288-2311.

Sekelsky, S.M., and R.E. McIntosh, 1996: Cloud Observations with a Polarimetric 33 GHz and 95 GHz Radar, *Meteorology and Atmospheric Physics*, 58, 123-140.

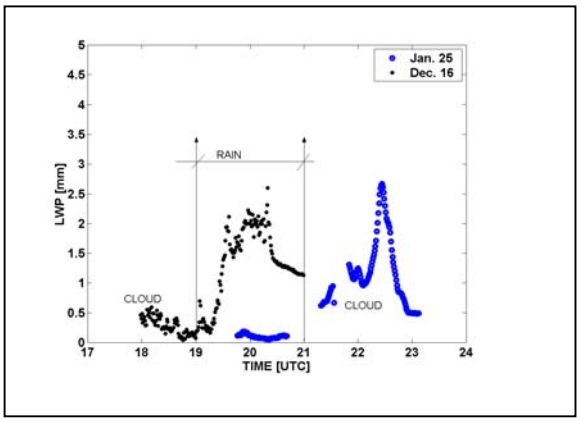

Fig. 1 LWP time series for Jan. 25 and Dec. 16 cases.

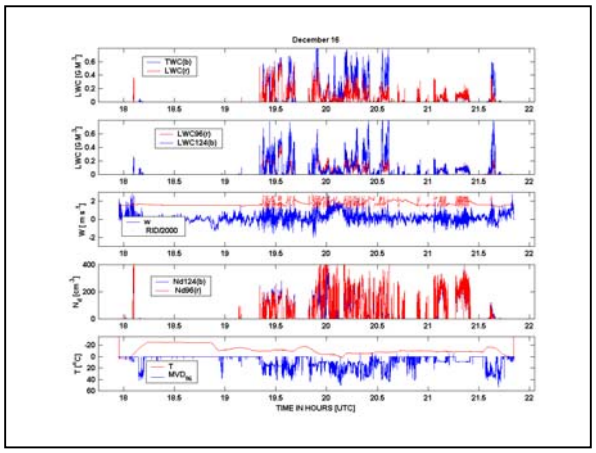

Fig. 2 Time series of in-situ observations for the Dec. 16 case. LWC from Nevzorov probes, LWC from FSSPs, vertical air velocity (w) and RID voltage, N_d, and T and r_{mvr} are shown in panels from top to bottom.

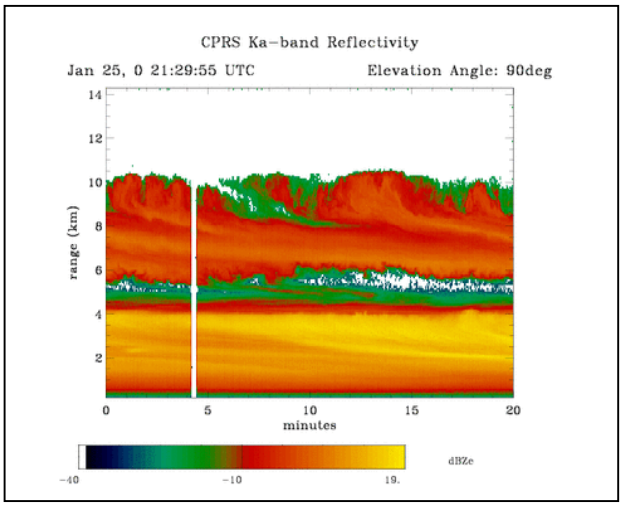

Figs. 3a: Time-height cross section of Z from CPRS Ka band radar.

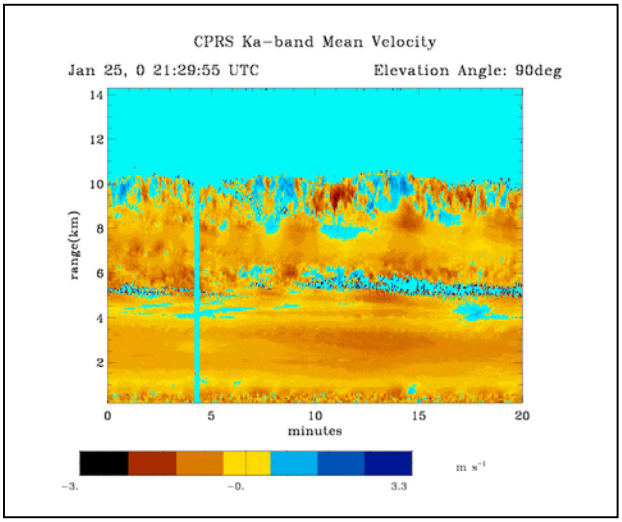

Figs. 3b: Time-height cross section of V_d from CPRS Ka band radar.

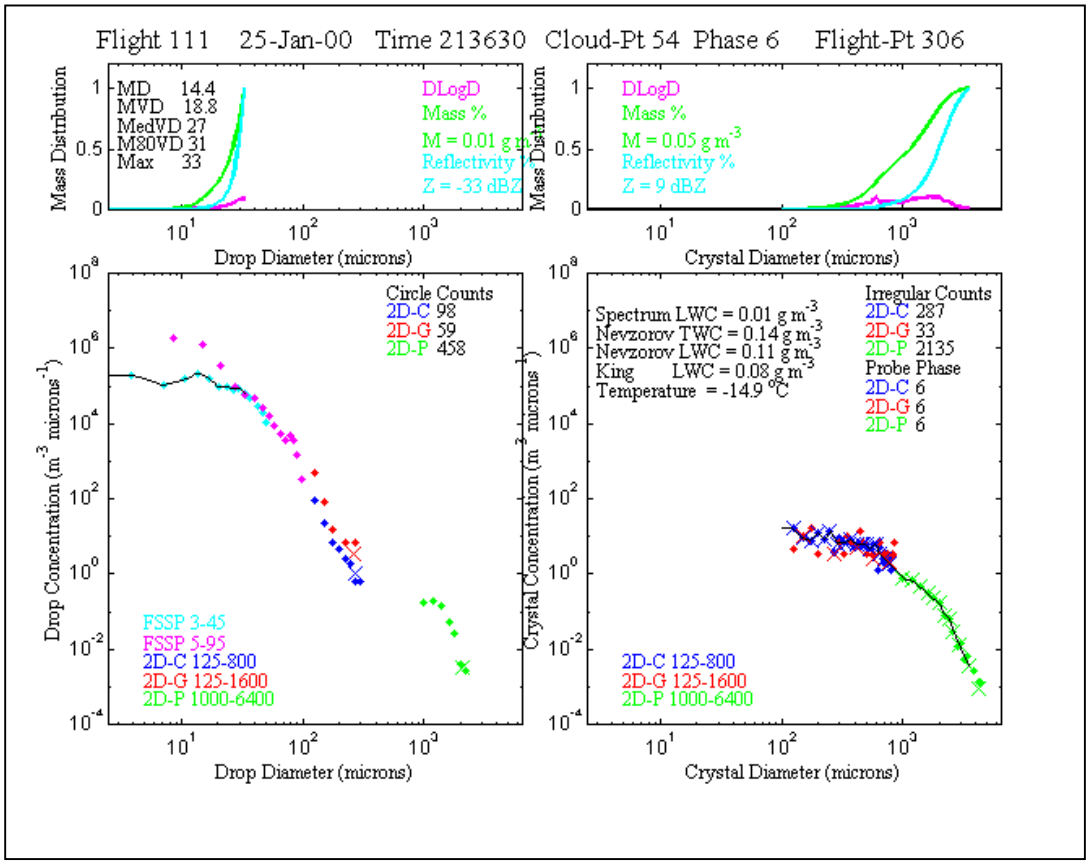

Fig. 4: Characteristics of microphysical data for the Jan. 25 case.

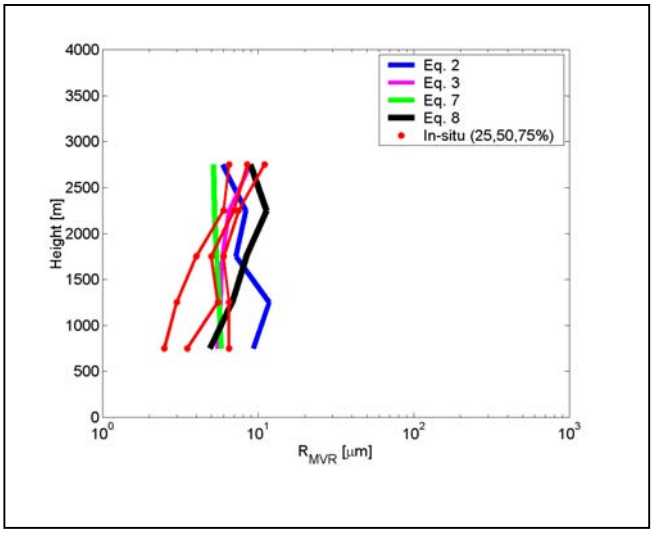

Fig. 5: Profiles of mean volume radius from various methods for the Dec. 16 case.

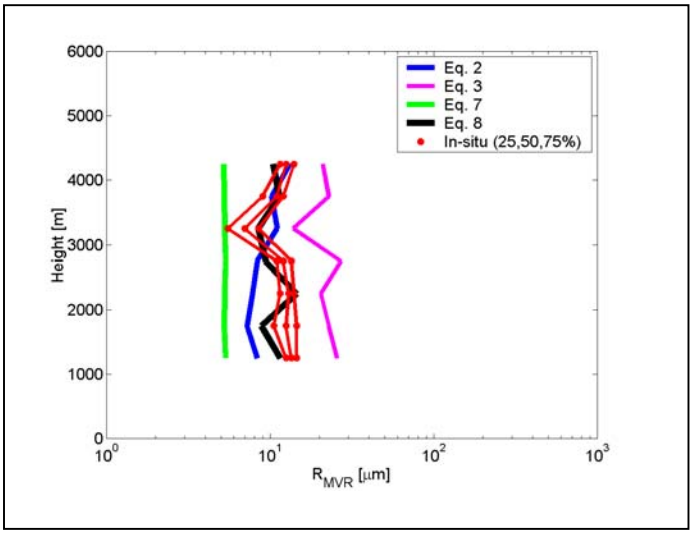

Fig. 6: Profiles of mean volume radius from various methods for the Jan. 25 case.